AUTHORS:
Chantal Tribolo[1]
Nicholas J. Conard[2,3]
Matthias Blessing[3,4]
Gregor D. Bader[2,5]

AFFILIATIONS:
[1]Archeosciences Bordeaux, CNRS, Bordeaux Montaigne University, Pessac, France
[2]Senckenberg Centre for Human Evolution and Palaeoenvironment, Tübingen, Germany
[3]Department of Geoscience, Early Prehistory and Quaternary Ecology, University of Tübingen, Tübingen, Germany
[4]Department of Anthropology, University of Connecticut, Storrs, Connecticut, USA
[5]Palaeo-Research Institute, University of Johannesburg, Johannesburg, South Africa

CORRESPONDENCE TO:
Chantal Tribolo

EMAIL:
ctribolo@u-bordeaux-montaigne.fr

DATES:
Received: 05 Sep. 2023
Revised: 08 Apr. 2024
Accepted: 17 Apr. 2024
Published: 31 July 2024

HOW TO CITE:
Tribolo C, Conard NJ, Blessing M, Bader GD. An updated chronology for Umbeli Belli and its implications for the Middle and Later Stone Ages. S Afr J Sci. 2024;120(7/8), Art. #16799. https://doi.org/10.17159/sajs.2024/16799

ARTICLE INCLUDES:
☒ Peer review
☐ Supplementary material

DATA AVAILABILITY:
☐ Open data set
☐ All data included
☒ On request from author(s)
☐ Not available
☐ Not applicable

EDITORS:
Jemma Finch
Tim Forssman

KEYWORDS:
luminescence dating, Middle Stone Age, Later Stone Age, lithic technology

FUNDING:
French National Research Agency (ANR-21-CE27-0030-001)

An updated chronology for Umbeli Belli and its implications for the Middle and Later Stone Ages

We present a series of 12 OSL/IRSL dates that revise and complete the chronology of the important Middle (MSA) and Later Stone Age (LSA) site Umbeli Belli in KwaZulu-Natal, South Africa. These dates shift the previous radiometric ages thousands of years older than earlier measurements and play a key role in revising the cultural stratigraphy of KwaZulu-Natal. We also discuss how these dates bring the chrono- and cultural stratigraphy of southern Africa into clearer focus. The Robberg sequence of Umbeli Belli is now firmly dated to 21 ± 2 ka, whereas the preceding Early LSA assemblage dates to ~32 ka, representing one of the earliest dates for this cultural expression in the broader region. The final MSA assemblages from Layer 7 to 9 now date to between 35 ka and 40 ka, overlapping more tightly with comparable assemblages from Sibhudu, Umhlatuzana and other sites. Layer 10, which was previously also assigned to the final MSA, now dates to ~47–54 ka, placing the assemblage within the temporal range of the Late MSA. The new dates provide a good explanation for the clear differences in material culture between Layer 10 and the younger layers. We also present two new ages for the deeper horizons 11b and 12 at Umbeli Belli, dating to 76 ± 9 ka and 80 ± 9 ka, respectively.

Significance:

- Revised and new age estimates are given for the Middle and Later Stone Age sequence of Umbeli Belli.
- These age changes allow new comparisons with nearby prehistoric sites.
- They change our view of the regional variability of technologies and cultures between ca. 80 and 20 ka on the east coast of South Africa.

Introduction

The Middle (MSA) and Later Stone Age (LSA) site of Umbeli Belli is a sandstone rock shelter situated on the east coast of South Africa, approximately 7 km inland from Scottburgh in KwaZulu-Natal. Charles Cable[1] (1984) initially excavated the site in 1979, with a research focus on the youngest occupation phase in Layer 1, 2BE and 2AL at the top of the sequence. Cable found a late expression of the LSA in those horizons associated with pottery and radiocarbon dates on charcoal falling between 200 ± 50 BP (Pta-2824) and 1140 ± 50 BP (Pta-2825).[2] Cable excavated the deeper deposits in four square metres, revealing a homogeneous orange-brown, compact sand with typical MSA tools. The assemblages in between the MSA and the Holocene LSA, later found during the Bader and Conard excavations, were not mentioned in Cable's 1984 publication. Due to Cable's research focus on later periods, he did not publish those assemblages until 2016 in connection with Bader's techno-typological study of this material. This research attributed the assemblage to the final MSA based on a regional comparison. Between 2016 and 2020, Bader and Conard, from the University of Tübingen, dug the site down to bedrock, revealing an unexpectedly long archaeological sequence encompassing a total of 15 geological horizons (GH).[2,3] These were subdivided by higher or lower amounts of sandstone roof spalls as well as by differences in texture, colour, and clast size. In the absence of organic material below Cable's Layer 2BE and 2AL, we conducted luminescence dating in the IRAMAT Laboratory (now renamed Archéosciences Bordeaux) of the University of Bordeaux Montaigne on single quartz grains and feldspar grains from nine samples (UBB1 to UBB9) for the GHs 3, 5, 7, 8, 9 and 10.[2] Table 8 of Bader et al.[2] presents the results of this first episode of luminescence dating. While the quartz and feldspar ages fell within one or two sigma uncertainties, we noticed that, except for one sample, the ages on feldspar were younger than the ages on quartz grains. We suspected that this may originate from an overestimate of the internal potassium (K) content of the feldspar grains.

According to those original dates, Umbeli Belli contains two Late Pleistocene LSA horizons, GH3 and GH5. GH3 was dated to 17.8 ± 1.5 ka. Blessing and colleagues[4] recently published the lithic assemblage from GH3 and assigned it to the Robberg technocomplex. While our study on GH5 is still in progress, we originally assigned GH7–GH10 to the Final MSA, dating at that time to between 29 ka and 40 ka.[2] In our recent study[5] we showed that the final MSA of GHs 7 and 8 at Umbeli Belli, dating between 29 ka and 32 ka, have strong affinities with the final MSA assemblages at Sibhudu dating to ~38 ka. The quartz ages from GHs 9 and 10 at Umbeli Belli previously fell between 32 ka and 40 ka and overlapped with the dates for the Final MSA from Sibhudu. However, GHs 9 and 10 from Umbeli Belli differ in their tool production, tool morphology and raw material economy from the Final MSA assemblages of Sibhudu. Based on these results, we concluded that the final MSA exhibits more regional and chronological variation than expected.[5]

In this paper we provide an updated chronology for Umbeli Belli. Based on a correction made on the beta source calibrations[6-9] for the artificial sources used to determine the equivalent doses, we show here that the quartz ages are 18% older than previously estimated, and that the consistency between the quartz and feldspar ages is improved. The hypothesis of internal K overestimation is no longer considered. This development has several important archaeological implications. Additionally, in 2019, we sampled three stratigraphic units – GH10, 11b and 12, which correspond to UBB10, 11 and 12 – in order to extend the chronology to the base of the sequence. We followed the same protocols as those employed for samples UBB1 to 9.

Old and new samples

Table 1 and Figure 1 display the locations for samples UBB1 to 9, previously published[2], and for samples UBB10 to 12, taken in 2019. They were taken at night, under subdued orange light, after discarding the surface of the section previously exposed to natural sunlight. The description of the geological horizons in which samples UBB1 to 9 were taken (GH3 to 10) can be found in Bader et al.[2] and will not be repeated here. UBB10, 11 and 12 come respectively from GH10 (as UBB 6), GH11b and 12. These layers are characterised as indicated below.

GH10: Munsell 5YR, 3/4. Dark reddish brown. Silty sand with a significant increase in quartzite spalls larger than 3 cm, mostly sharp edged and irregularly oriented in the sediment. Increase in artefact density.

GH11b: Munsell 7.5YR, 3/4. Dark brown. Silty sand. Well sorted without inclusion. Large amounts of flat oriented quartzite spall. Very high artefact density.

GH12: Munsell 5YR, 3/4. Dark reddish brown. Silty sand. Not well sorted with several inclusions. Considerably less quartzite spall compared to GH11b. High artefact density.

Methods

The luminescence dating method was applied to quartz and feldspar grains extracted from the sediment samples. This method exploits the ability of these minerals to act as rechargeable batteries: when submitted to radiative energy (from natural uranium series, thorium series, potassium content in the ground and from cosmic radiations), they can store it until they are exposed to light. This exposure frees the energy in the form of light, so that the amount of light is directly related to the amount of absorbed energy. The age of the sediment deposit, i.e. the age of the last exposure of the grains to sunlight, is the ratio of the equivalent dose (total amount of energy absorbed during burial) measured in the laboratory thanks to light stimulation to the dose rate (the rate at which the energy was absorbed), related mainly to the radioisotopic content in the ground and to the burial depth.

Revision of beta source calibration

The ages for UBB1 to 9 have been revised due to an improvement in the beta source calibration. The equivalent dose of a quartz or feldspar mineral is obtained by comparing the natural luminescence of the sample to the one induced by an artificial beta (or gamma) source. Therefore,

Table 1: Location of all luminescence dating samples from the site

Sample UBB	ID	Profile	Square	Z (cm)	Geological horizon
1	2578	East	3/13	17.386	9
2	19	East	3/12	17.599	8
3	18	East	3/12	17.749	7
4	100	North	2/15	17.957	7
5	99	North	2/15	18.508	3
6	92	North	2/15	17.297	10
7	95	North	2/15	17.776	8
8	98	North	2/15	18.335	5
9	17	East	3/12	17.994	5
10	41	South	3/12	17.164	10
11	42	South	3/12	16.955	11b
12	43	South	3/12	16.694	12

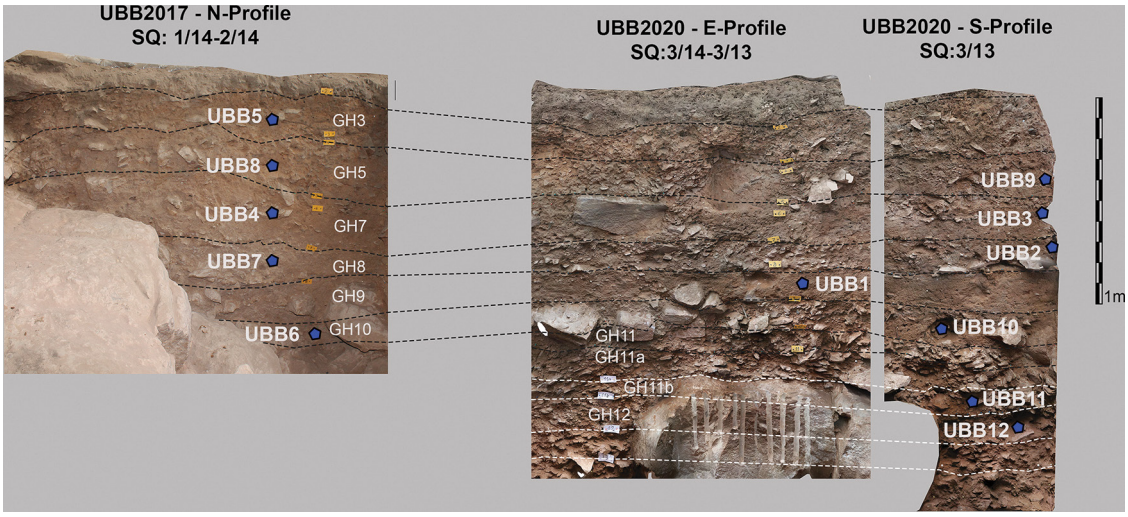

Figure 1: Photographs of the stratigraphic sections displaying the location of the luminescence dating sediment samples.

what is measured is actually first an equivalent time of irradiation. The equivalent dose in gray (Gy) is the following product:

Equivalent dose (Gy) = (equivalent time of irradiation for the sample, s) x (source dose rate, Gy/s).

In order to determine the source dose rate, laboratories use quartz grains whose absorbed dose is certified, and look for the corresponding equivalent time of irradiation:

Source dose rate (Gy/s) = (certified equivalent dose, Gy) / (equivalent time of irradiation for the certified quartz, s).

Therefore, any mistake on the certified equivalent dose will be directly reported on the sample equivalent dose, and on the age.

In 2019, Tribolo et al.[6], using quartz irradiated with three different gamma sources (i.e. different certified calibration quartz), observed a significant 14% difference between the estimated beta source calibrations for the same beta source. Additional work performed by the calibration quartz providers showed that the dose for the Risø calibration quartz had actually been miscalculated. It was shown that: (1) the equation for calculating the dose was incomplete (neither the contribution from build-up of scattered photon in the irradiation cell, nor the contribution from build-up in air, or backscattering from the support material had been taken into account), and (2) the distance between the gamma source and the calibration sample had not been perfectly controlled, inducing variabilities from batch to batch.[7,9]

In our laboratory, over the years, we have used several batches of Risø calibration quartz (RCQ) together with several batches of Lexcal quartz (LCQ) in order to calibrate our readers. The mean beta source calibration for each reader was not necessarily calculated from the same sets of batches. In some cases, instead of applying the beta source calibration from RCQ or LCQ, we applied the beta source calibration calculated using the sample to be dated, bleached and gamma irradiated at the Laboratoire des Sciences du Climat et de l'Environnement (LSCE, Gif-sur Yvette, France)[e.g.10]. However, this was not the case for Umbeli Belli: quartz and feldspar single-grain equivalent doses were measured on two different devices, calibrated with different RCQ and LCQ batches, inducing dispersions within the ages. As it is clear now that the RCQ absorbed dose was miscalculated, we have been able to correct the calibration dose rate for each reader, based on the LSCE-irradiated quartz and LCQ, and then correct the ages for the samples from Umbeli Belli.

Dating of additional samples

Quartz grains were extracted using mechanical and chemical processes: wet sieving in order to extract the 100–140-µm grain size, HCl (10%) and H_2O_2 (30%) for carbonate and organic material removal, followed by heavy liquid separation with heteropolytungstate of sodium at 2.72 g/cm^3 and 2.62 g/cm^3. Quartz grains were then HF etched (40% for 1 h, followed by HCl).

The extracted 100–140-µm quartz grains were then mounted on single-grain discs with 100 cylindrical holes, 150 µm diameter and 150 µm deep. Infrared-stimulated luminescence (IRSL) tests following Duller[11] were performed in order to check the absence of any contaminant feldspar grain. Measurements for the equivalent dose (De) determination were performed on a single-grain Risø reader (the same as the one used for UBB1 to UBB9). This TL-DA 20 Risø reader is equipped with a EMI ET 9107 PM tube (erroneously called Q9235 in the previous paper[2]) preceded by a 7.5 mm Hoya U340 filter for detection in the UV (280–380 nm) while excitation is performed with a green laser (532 nm).[12,13] Analyst v.4.57[14] was used for analyses.

The single-aliquot regenerative-dose protocol (SAR[15]) was performed (Figure 2), with the same preheat parameters as those applied to UBB1 to 9. The efficiency of the protocol (i.e. its suitability to recover at least a known laboratory-given dose) was checked with dose recovery tests (Table 2). Growth curves were fitted with saturating exponential ($y = a[1-\exp[[x+b] / D_0]]]$, where y is the sensitivity corrected signal, x is the dose, and a, b and D_0 are fitting parameters). The criteria for grain selection were, again, the same as the ones applied to samples UBB1 to UBB9: (1) natural test dose signal >3 sigma of the mean background signal, (2) recuperation [0 Gy dose] signal <5% of natural signal, (3) natural test dose relative uncertainty <10%, (4) natural signal under the saturation level (i.e. a De can be calculated with a finite uncertainty), and (5) application of a D_0 threshold, following Thomsen et al.[16] These authors have shown that the De values for grains with early saturation (i.e. low D_0 values) are systematically underestimated and must be excluded before calculating the final CAM (Central Age Model[17]) De (or any other statistical model). The De values are then ranked by increasing D_0 value, and the CAM is calculated after progressively discarding the De_s below the D_0 threshold. Typically, an increase in the CAM De value is observed until a plateau is reached. In our case, we also observed the percentage of grains that passed selection criteria 1–3 but were rejected

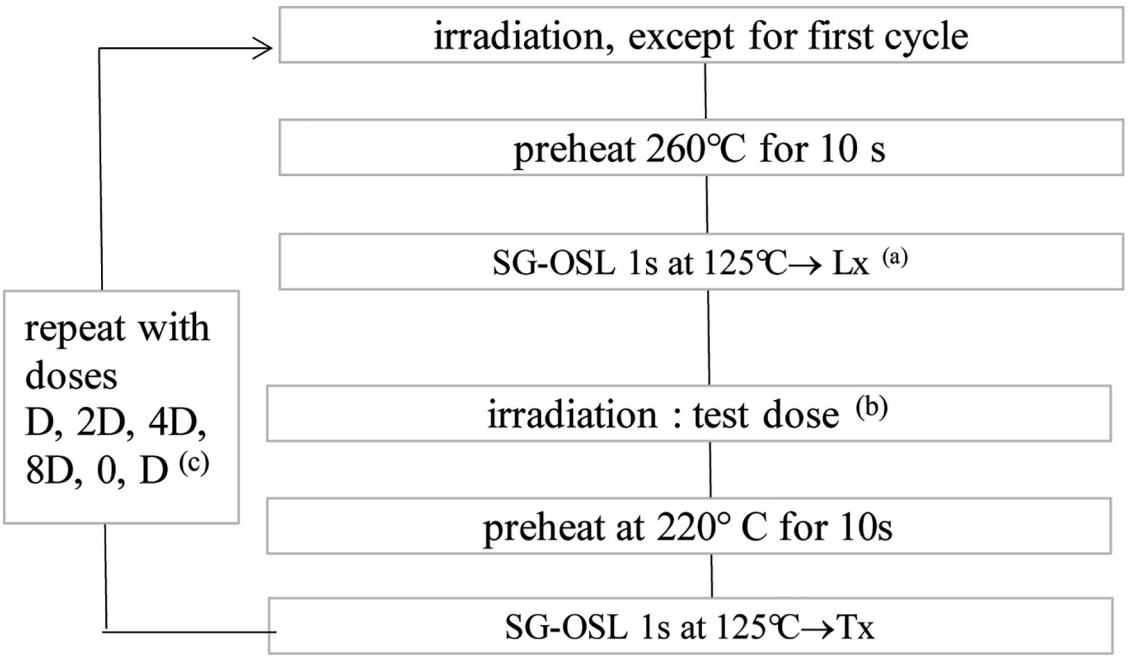

Figure 2: Single-aliquot regenerative-protocol applied to the 100–140-µm quartz grains. (a) The first 0.05 s and last 0.10 s were used for signal and background, respectively. (b) The test dose was 43 Gy for UBB10 and 11 and 73 Gy for UBB12. (c) D was 43 Gy for UBB10 and UBB11, and 73 Gy for UBB12.

because of saturation as a function of the D_0 threshold. The D_0 threshold (and corresponding CAM De) is chosen where the plateau is reached and the percentage of rejected grains is below 5%.

The total dose rate is the sum of the contributions from the cosmic, gamma, beta and alpha dose rates. The cosmic dose rates (Dr) were based, as for UBB1 to 9, on the equation of Prescott and Hutton[18], taking into account the burial depth, geographic coordinates, and geometry of the shelter. The gamma dose rates were measured with Al_2O_3:C dosimeters, following Kreutzer et al.[19,20] The beta dose rates were calculated from the radioisotopic contents of the samples, using the conversion factors and attenuation factors of Guérin et al.[21,22] For the previous analysis of samples UBB 1 to 9, the radioisotopic contents had been measured with high-resolution gamma spectrometry on ca. 20 g of the sample, dried, finely crushed and sealed with wax in a plastic box. This was done separately on fractions <2 mm and 2 mm–1 cm, in order to calculate beta dose rate from the 'fine fraction' (<2 mm) and from the 'total' (actually <1 cm) fraction. It has been shown that, in theory, because of the ca. 2 mm travel range of beta particles and the resulting auto-absorption for various grain sizes, the true beta dose rate must be bracketed by these two beta dose rate estimates.[23,24] However, we observed that, in the case of UBB1 to 9, there was little (negligible) variation between the two beta dose rate estimates. Therefore, for samples UBB10 to 12, the radioisotopic contents were measured on the <2 mm fraction only. The alpha dose rate was assumed to be negligible due to the HF etching. The same correction for water content was applied (mean moisture 5.0% ± 1.5%) as for the previous series of samples.

Results

Revision of ages for UBB1–9

Table 3 presents the previous and revised ages based on the revised calibration dose rates. For the quartz samples, the beta source calibration was estimated, at the time of measurement, for 300-µm-hole SG discs, as 0.126 Gy/s instead of 0.107 Gy/s. For the feldspar grains, measured on a second device, it was estimated as 0.144 Gy/s instead of 0.107 Gy/s. With the previous calibration estimates, the ratio of feldspar to quartz ages was within one or two sigma, but between 0.99 and 1.30 (with a mean of 1.13). Now the ratios are between 0.87 and 1.14 (with a mean of 0.99), showing that we still have good agreement but no longer a systematic trend.

Additional age estimates for UBB10–12

The cosmic, gamma and beta dose rates for samples UBB10, 11 and 12 are shown in Table 4. Table 5 displays the corresponding K, U and Th activities or contents. Note that the K, Th and bottom of U chain (^{210}Pb) contents or activities for UBB10 are within 5% of those for UBB6, from the same unit (the head and middle of the chain are slightly different, within 21 and 8% of those for UBB6, although consistent at two sigma). No significant disequilibrium in the U chain is observed for the three samples. The total dose rates for samples UBB10 to UBB12 are between 2.69 ± 0.18 Gy/ka and 3.21 ± 0.21 Gy/ka for the 100–140 µm quartz grains, which is similar or slightly higher than the dose rates for samples UBB1 to UBB9.

Table 2: Results for the dose recovery tests. The samples were bleached for 1 min in a solar simulator (Holne UVACube 400, left in the dark for at least 10 000 s and bleached for 200 s in the reader (blue stimulation) at room temperature). N measured: total number of measured grains; Pass crit 1–3 or crit1–4: number of selected grains that pass criteria 1 to 3 or 1 to 4, as described in the main text; After D_0: number of selected grains that pass criteria 1–5; DRT-CAM: ratio of measured to given equivalent dose after the central age model[18]; OD: overdispersion.

Sample	Given dose (Gy)	N measured	Pass crit 1–3	Pass crit 1–4	After D_0	D_0 (Gy)	DRT-CAM		OD (%)	
UBB10	149	800	133	96	21	148	0.98	± 0.03	8	± 4
UBB11	149	800	122	96	20	148	0.96	± 0.02	5	± 3
UBB12	260	800	127	65	12	200	0.94	± 0.03	0	

Table 3: In chrono-stratigraphic order from the top to the bottom of the sequence, previously published[2] and recalculated ages for samples UBB1 to UBB9 based on revised beta source calibrations. The last rows present the additional ages for UBB10 to UBB12, based on the data presented in Tables 4–6.

Sample	Geological horizon	Age – old (ka)				Age – new (ka)			
		Quartz		Feldspar		Quartz		Feldspar	
UBB5	3	17.8	± 1.5	–	–	**21**	**± 2**	–	–
UBB8	5	27.2	± 2.3	21	± 1.4	**32**	**± 3**	**28**	**± 2**
UBB9	5	24.9	± 2.3	22.7	± 1.8	**29**	**± 3**	**31**	**± 3**
UBB3	7	28.1	± 2.2	–	–	**33**	**± 3**	–	–
UBB4	7	29.9	± 2.3	28.9	± 1.8	**35**	**± 3**	**39**	**± 3**
UBB2	8	32.2	± 2.6	27.8	± 2.2	**38**	**± 3**	**37**	**± 3**
UBB7	8	31.5	± 2.5	31.8	± 2.4	**37**	**± 3**	**43**	**± 3**
UBB1	9	32.9	± 2.5	30.2	± 2.7	**39**	**± 3**	**41**	**± 4**
UBB6	10	40.3	± 3.5	32.5	± 3.0	**47**	**± 4**	**44**	**± 4**
UBB10	10	–	–	–	–	**54**	**± 5**	–	–
UBB11	11b	–	–	–	–	**76**	**± 9**	–	–
UBB12	12	–	–	–	–	**80**	**± 9**	–	–

Table 4: Dose rate data for the previously published data and for the new samples. Water content: mean mass of water over the mass of dry sediment; Coarse: mass of 2 mm–1 cm material over the mass of <1 cm dry sediment; Beta 1: beta dose rate calculated from the content in the <2 mm fraction; Beta 2: beta dose rate calculated from the content in the 2 mm–1 cm fraction.

Sample	Grain size (μm)	Content		Dose rate (gy/ka)								Total dose rate (gy/ka)	
		Water	Coarse	Cosmic		Gamma		Beta 1		Beta 2			
UBB1	200–250	5%	7%	0.12	± 0.01	1.14	± 0.06	1.62	± 0.15	1.60	± 0.15	2.88	± 0.17
UBB2	200–250	5%	9%	0.12	± 0.01	1.04	± 0.07	1.51	± 0.14	1.49	± 0.14	2.67	± 0.16
UBB3	200–250	5%	6%	0.12	± 0.01	1.05	± 0.06	1.52	± 0.14	1.51	± 0.14	2.69	± 0.16
UBB4	200–250	5%	5%	0.12	± 0.01	0.99	± 0.05	1.53	± 0.15	1.53	± 0.15	2.65	± 0.16
UBB5	200–250	5%	5%	0.12	± 0.01	0.98	± 0.11	1.59	± 0.16	1.58	± 0.16	2.69	± 0.19
UBB6	200–250	5%	10%	0.12	± 0.01	0.94	± 0.10	1.68	± 0.16	1.67	± 0.16	2.74	± 0.19
UBB7	200–250	5%	7%	0.12	± 0.01	1.00	± 0.07	1.59	± 0.15	1.59	± 0.15	2.71	± 0.17
UBB8	200–250	5%	11%	0.12	± 0.01	0.87	± 0.08	1.44	± 0.14	1.28	± 0.13	2.36	± 0.16
UBB9	200–250	5%	22%	0.12	± 0.01	0.87	± 0.10	1.60	± 0.15	1.56	± 0.15	2.57	± 0.18
UBB10	**100–140**	**5%**	**16%**	**0.12**	**± 0.01**	**0.83**	**± 0.06**	**1.74**	**± 0.17**			**2.69**	**± 0.18**
UBB11	**100–140**	**5%**	**21%**	**0.12**	**± 0.01**	**1.19**	**± 0.15**	**1.88**	**± 0.18**			**3.19**	**± 0.23**
UBB12	**100–140**	**5%**	**13%**	**0.12**	**± 0.01**	**1.10**	**± 0.07**	**1.99**	**± 0.19**			**3.21**	**± 0.21**

Table 5: Radioisotope activities (for U and Th series) or contents (for K) of samples UBB10 to 12. All data were calculated from high-resolution gamma spectrometry measurements.

Sample	Activities (Bq/kg)								Content (%)	
	^{238}U series						^{232}Th series		K	
	(^{234}Th)		(^{226}Ra)		(^{210}Pb)					
UBB10	34.56	±5.12	33.08	±1.20	34.84	±2.01	39.49	±4.26	1.67	±0.03
UBB11	38.86	±6.12	33.86	±1.27	39.89	±2.22	45.25	±5.42	1.79	±0.03
UBB12	38.85	±6.37	33.40	±1.27	39.39	±2.27	44.48	±5.42	1.95	±0.03

Figure 3 displays the De-D_0 plots for samples UBB10–12. The overdispersion (54 ± 6% to 60 ± 5%) is as high or slightly higher than that observed for UBB1–9 (32 ± 3% to 53 ± 4%). For these samples, the average dose model (ADM, Guérin et al.[25]) had been applied, assuming well-bleached, undisturbed samples (note that the debate about the accuracy of the statistical models is still pending; choosing the CAM (Central Age Model)[18] would give slightly lower equivalent doses and ages). For sample UBB9 in particular (OD 53 ± 4%), there is a good agreement between quartz and feldspar ages, and no chronostratigraphic reversal, suggesting that this higher OD might be due to microdosimetric effects. While this finding will be investigated further in the near future, we have assumed it is also the case for samples UBB10–12. Therefore, we have applied the same statistical model. The equivalent dose is 145.0 ± 7.8 Gy for UBB10 and is significantly higher for UBB11 and UBB12 from the lower layers (242.9 ± 20.1 Gy and 257.3 ± 21.1 Gy, respectively) (Table 6).

The quartz ages are 54 ± 5 ka for UBB10, 76 ± 9 ka for UBB11, and 80 ± 9 ka for UBB12. We note that the quartz age of UBB10 is slightly higher than the quartz and feldspar ages of UBB6, from the same horizon (47 ± 4 ka and 44 ± 4 ka, respectively), although consistent at 2 sigma. All ages are displayed in Figure 4.

Discussion and conclusion

The corrected age model for Umbeli Belli leads to several changes in our understanding of the chrono-cultural sequence of the MSA and LSA in the eastern part of southern Africa.

Table 3 provides the old and new dates for the quartz and feldspar grains. These results show that GH3, formerly dated to 17.8 ± 1.5 ka, now dates to 21 ± 2 ka. The assemblage from GH3 was recently published by Blessing et al.[4] and assigned to the Robberg technocomplex. Considering the new age for GH3, the Robberg assemblage from Umbeli Belli now counts among the oldest in southern Africa, together with, for example, Heuningneskrans[26], Elands Bay[27] and Boomplaas[28]. This does not affect the designation of the GH3 lithic assemblage as belonging to the Robberg technocomplex, but shows that an early onset of this technocomplex might have been more widespread than previously thought.

GH5 dates now to between 28 ± 2 ka and 32 ± 3 ka. The assemblage from this horizon was recently analysed and those results published in a separate article.[3] The lithic assemblages of GH4 and GH6, which are not dated, also form part of this study. These assemblages show features of Early LSA or MSA/LSA transitional industries, the likes of which were also found at Rose Cottage Cave and Umhlatuzana.[29,30] While undated, GH4 and GH6 are stratigraphically bracketed between the dated Layers 3 and 5, and 5 and 7, respectively. Blessing et al.[3] observed gradual changes rather than abrupt breaks in lithic technology between those GHs. Despite this continuity reflected in lithic technology, the luminescence dates indicate a chronological gap between the GH7–5 assemblages and the Robberg assemblage of GH3, which may reflect a hiatus in the site's occupation. However, this question must remain unresolved at the moment, due to the absence of dating results from GH4.

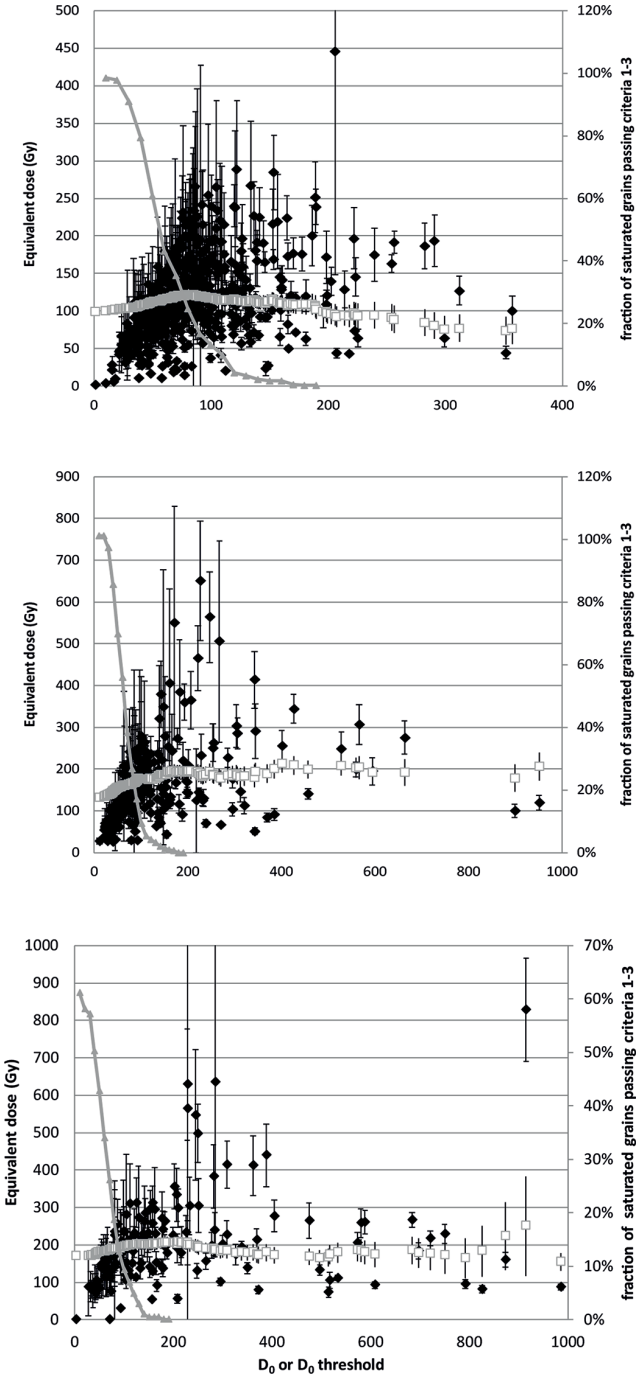

Figure 3: De-D_0 plot for UBB10 (top), UBB11 (middle), UBB12 (bottom). Black diamonds: equivalent doses plotted against the corresponding D_0 value. White squares: Central Age Model (CAM) value in function of the lowest D_0 included in the selection (i.e. only the De values corresponding to the black diamonds above the D_0 threshold are considered in the distribution for calculating the CAM De). Grey triangles represent the percentage of saturated grains (secondary *y*-axis) which pass selection criteria 1–3 after exclusion of grains below a Do threshold (*x*-axis).

Table 6: Data for the equivalent doses of samples UBB10 to UBB12. N measured: total number of measured grains; Pass crit 1–3 or crit 1–4: number of selected grains that pass criteria 1 to 3 or 1 to 4, as described in the main text; After D_0: number of selected grains that pass criteria 1–5; De (Gy)-CAM: equivalent dose after the Central Age Model; OD: overdispersion; De (Gy)-ADM: equivalent dose after the Average Dose Model; Sigma D: overdispersion associated with ADM De, after taking into account the sigma_m dispersion due to the measurement in addition to the statistical dispersion. The ADM is calculated for an assumed sigma_m value of 15%. However, the ADM De is insensitive to sigma-m in the range 5–15%.

Sample	N measured	Pass crit 1–3	Pass crit 1–4	After D_0	D_0 (Gy)	De (Gy)-CAM		OD (%)		De (Gy)-ADM		Sigma D (%)	
UBB10	6700	617	492	83	130	122.8	± 8.3	60	± 5	145.0	± 7.8	58	± 7
UBB11	2400	578	240	46	180	212.1	± 17.8	54	± 6	242.9	± 20.1	52	± 6
UBB12	2400	357	151	53	200	224.5	± 17.7	54	± 6	257.3	± 21.1	52	± 6

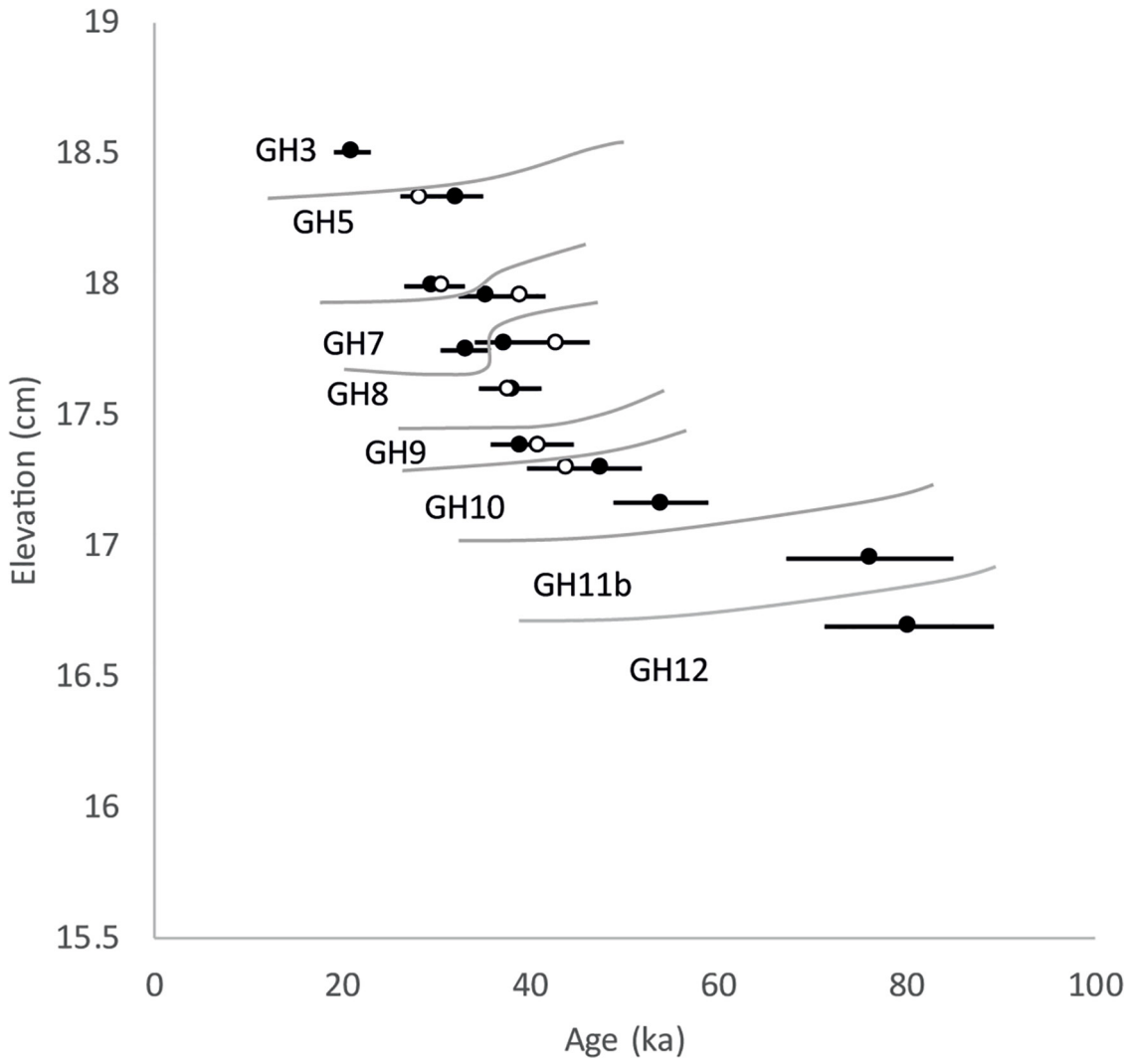

Figure 4: Summary of the ages for Umbeli Belli in relation to the elevation of the sample. Black dots: quartz ages; white dots: feldspar ages. The grey lines are arbitrarily drawn in order to highlight the geological horizon (GH) attribution of each sample. Variability in elevation is due to both GH thickness and slope at the site.

The assemblages of GH7–10 were formally assigned to the final MSA. In our recent comparative study between Sibhudu[5] and Umbeli Belli[2], we observed considerable differences in GH7 and GH8 compared to GH9 and GH10 at Umbeli Belli. We attributed these differences to natural inter- and intra-site variability, potentially linked to changes in raw material availability related to changes in sea level stand, insolation and river erosional processes. However, with respect to the new dating results, we must step back from those earlier conclusions. In fact, GH7 and GH8 now overlap well with the final MSA assemblages from Sibhudu[31] and Umhlatuzana[32-34], both in lithic artefact composition and dating. They include bifacial technology, basal thinning, a high number of shaping flakes and the presence of hollow-based points and segments (the latter two only in GH7 of Umbeli Belli) – all attributes that were recently described as characteristics of the Eastern final MSA.[5] GH9 and GH10 showed the biggest differences from the Sibhudu final MSA, namely: an absence of basal thinning, hollow-based points, shaping technology, segments and a completely different signal in raw material economy (sandstone vs hornfels). The new dating results push GH9 and GH10 back several millennia, offering a decent explanation for differences observed in the archaeological signal. Layer 10, in particular, now overlaps more in time with the assemblages assigned to the Late MSA at Sibhudu.[35,36] According to Villa and colleagues[36], the Late MSA assemblage from Layer RSP contains mostly unifacial pointed forms and only occasional bifacial components. No hollow-based points or segments were found in those layers, but several scrapers were found. Those are features which were also found in GH10 at Umbeli Belli. Notably, the description of several cores in Layer RSP reflects exactly the definition of the final MSA cores we published in Bader et al.[2(p.18)]. Villa et al.[36(p.405)] write:

> *Cores with recurrent unidirectional or bidirectional flaking on a relatively flat surface with simply prepared striking platforms (n = 6). Sometimes the debitage surface and the striking platform are inverted during debitage. With one exception (Fig. 6 (1)) there are no traces of core surface shaping, prior to removal; the lateral convexities are maintained by the removal of flakes with a cortical back from the core margins.*

We identified such cores within GH7–10 at Umbeli Belli and within the final MSA layers Coffee to Espresso at Sibhudu. In the light of the new dating results presented above, we now have clear indication that this tradition of core reduction observed in the final MSA might have its roots several millennia earlier. The tool description of the Late MSA of Sibhudu also overlaps well with GH10 at Umbeli Belli. Thus, both our updated chronology and similarities in technology and typology, clearly indicate that GH10 needs to be assigned to an earlier phase of the MSA, and we tend to use Wadley's term 'Late MSA' at this stage of research.

Ultimately, the two new ages for GH11b and GH12 at the bottom of the sequence fall within an interesting time frame, overlapping with dating results for Still Bay and Howiesons Poort assemblages

in different parts of the subcontinent. No detailed observations on the lithic assemblages of those horizons have been published yet, but preliminary observations indicate a picture different from what conventionally would be expected.

The revised chronology of Umbeli Belli proves once more the importance of the site in the light of constant attempts to further structure and sharpen our understanding of spatio-temporal expressions of human material culture and behaviour, now reaching back to 80 000 years.

Acknowledgements

We are grateful to Chief Cele and the members of the Cele tribal council for allowing our team to conduct research at Umbeli Belli, which is on their land. We thank all the members of the field and laboratory crew; Dr Gavin Whitelaw and the staff of the KwaZulu-Natal Museum for generously providing storage and laboratory space and logistical support; and Amafa for providing the research permits for Umbeli Belli.

Funding

The OSL analyses were funded by the ANR project 'The MileStone Age' (ANR-21-CE27-0030-001).

Data availability

Data are available upon request to the corresponding author.

Declaration of AI use

AI was not used in the preparation of this paper.

Authors' contributions

C.T.: Data collection, data analysis, writing – initial draft, funding acquisition. N.J.C: Project leadership, funding acquisition, writing – initial draft. M.B.: Writing – initial draft. G.D.B.: Project leadership, writing – initial draft. All authors read and approved the final manuscript.

Competing interests

We have no competing interests to declare.

References

1. Cable C. Economy and technology in the late Stone Age of southern Natal. Cambridge Monographs in African Archaeology. Oxford: BAR Publishing; 1984. https://doi.org/10.30861/9780860542582
2. Bader G, Tribolo C, Conard N. A return to Umbeli Belli: New insights of recent excavations and implications for the final MSA of eastern South Africa. J Archaeol Sci Rep. 2018;21:733–757. https://doi.org/10.1016/j.jasrep.2018.08.043
3. Blessing MA, Conard, NJ, Bader, GD. Cultural developements between the Final MSA and the Robbergat Umbeli Belli, South Africa. J Paleo Arch. 2023;6–31. https://doi.org/10.1007/s41982-023-00161-z
4. Blessing MA, Conard NJ, Bader GD. Investigating the MIS2 microlithic assemblage of Umbeli Belli rockshelter and its place within the chrono-cultural sequence of the LSA along the East Coast of southern Africa. Afr Archaeol Rev. 2023;40:145–167. https://doi.org/10.1007/s10437-022-09497-3
5. Bader GD, Sommer C, Conard NJ, Wadley L. The final MSA of eastern South Africa: A comparative study between Umbeli Belli and Sibhudu. AZANIA. 2022;57(2):197–238. https://doi.org/10.1080/0067270X.2022.2078553
6. Tribolo C, Kreutzer S, Mercier N. How reliable are our beta-source calibrations? Ancient TL. 2019;37:1–10.
7. Hansen V, Murray A, Buylaert JP, Yeo EY, Thomsen K. A new irradiated quartz for beta source calibration. Radiat Meas. 2015;81:123–127. https://doi.org/10.1016/j.radmeas.2015.02.017
8. Richter D, Woda C, Dornich K. A new quartz for γ-transfer calibration of radiation sources. Geochronometria. 2020;47(1):23–34. https://doi.org/10.2478/geochr-2020-0020
9. Autzen M, Andersen CE, Bailey M, Murray AS. Calibration quartz: An update on dose calculations for luminescence dating. Radiat Meas. 2022;157, Art. #106828. https://doi.org/10.1016/j.radmeas.2022.106828
10. Tribolo C, Mercier N, Douville E, Joron J-L, Reyss J-L, Rufer D, et al. OSL and TL dating of the Middle Stone Age sequence of Diepkloof Rock Shelter (Western Cape, South Africa): A clarification. J Archaeol Sci. 2013;40(9):3401–3411. https://doi.org/10.1016/j.jas.2012.12.001
11. Duller GAT. Distinguishing quartz and feldspar in single grain luminescence measurements. Radiat Meas. 2003;37:161–165. https://doi.org/10.1016/S1350-4487(02)00170-1
12. Bøtter-Jensen L, Bulur E, Duller GAT, Murray AS. Advances in luminescence instrument systems. Radiat Meas. 2000;32:523–528. https://doi.org/10.1016/S1350-4487(00)00039-1
13. Bøtter-Jensen L, Andersen CE, Duller GAT, Murray AS. Developments in radiation, stimulation and observation facilities in luminescence measurements. Radiat Meas. 2003;37:535–541. https://doi.org/10.1016/S1350-4487(03)00020-9
14. Duller GAT. The Analyst software package for luminescence data: Overview and recent improvements. Ancient TL. 2015;33(1):35–42.
15. Murray AS, Wintle AG. Luminescence dating of quartz using an improved single-aliquot regenerative-dose protocol. Radiat Meas. 2000;32:57–73. https://doi.org/10.1016/S1350-4487(99)00253-X
16. Thomsen K, Murray AS, Buylaert JP, Jain M, Hansen JH, Aubry T. Testing single-grain quartz OSL methods using sediment samples with independent age control from the Bordes-Fitterockshelter (Roches d'Abilly site, Central France). Quat Geochronol. 2016;31:77–96. https://doi.org/10.1016/j.quageo.2015.11.002
17. Galbraith RF, Roberts RG, Laslett GM, Yoshida H, Olley JM. Optical dating of single and multiple grains of quartz from Jinmium rock shelter, northern Australia, Part I: Experimental design and statistical models. Archaeometry. 1999;41(2):339–364. https://doi.org/10.1111/j.1475-4754.1999.tb00987.x
18. Prescott JR, Hutton JT. Cosmic ray contributions to dose rates for luminescence and ESR dating: Large depths and long-term time variations. Radiat Meas. 1994;23:497–500. https://doi.org/10.1016/1350-4487(94)90086-8
19. Kreutzer S, Tribolo C, Martin L, Mercier N. Dose-rate estimation using α-Al2O3:C chips: Aftermath. Ancient TL. 2020;38:1–10.
20. Kreutzer S, Martin L, Tribolo C, Selva P, Mercier N. Environmental dose rate determination using a passive dosimeter: Techniques and workflow for α-Al2O3:C chips. Geochronometria. 2018;45:56–67. https://doi.org/10.1515/geochr-2015-0086
21. Guérin G, Mercier N, Adamiec G. Dose rate conversion factors: Update. Ancient TL. 2011;29:5–8.
22. Guérin G, Mercier N, Nathan R, Adamiec G, Lefrais Y. On the use of the infinite matrix assumption and associated concepts: A critical review. Radiat Meas. 2012;47:778–785. https://doi.org/10.1016/j.radmeas.2012.04.004
23. Martin L. Caractérisation et modélisation d'objets archéologiques en vue de leur datation par des méthodes paléo-dosimétriques. Simulation des paramètres dosimétriques sous Geant4 [Characterization and modeling of archaeological objects with a view to their dating using paleo-dosimetric methods. Simulation of dosimetric parameters under Geant4] [unpublished PhD thesis].Pessac: University of Bordeaux Montaigne; 2015.
24. Tribolo C, Asrat A, Bahain J-J, Chapon C, Douville E, Fragnol C, et al. Across the gap: Geochronological and sedimentological analyses from the late Pleistocene-Holocene sequence of Goda Buticha, southeastern Ethiopia. PLoS ONE. 2017;12(1), e0169418. https://doi.org/10.1371/journal.pone.0169418
25. Guérin G, Christophe C, Philippe A, Murray AS, Thomsen KJ, Tribolo C, et al. Absorbed dose, equivalent dose, measured dose rates, and implications for OSL age estimates: Introducing the Average Dose Model. Quat Geochronol. 2017;41:163–173. https://doi.org/10.1016/j.quageo.2017.04.002
26. Beaumont P. The Heuningneskrans Shelter. In: Voigt EA, editor. Guide to archaeological sites in the Northern and Eastern Transvaal. Pretoria: Transvaal Museum; 1981. p. 132–145.
27. Porraz G, Igreja M, Schmidt P, Parkington JE. A shape to the microlithic Robberg from Elands Bay Cave (South Africa). South Afr Humanit. 2016;29(1):203–247.
28. Pargeter J, Loftus E, Mackay A, Mitchell P, Stewart B. New ages from Boomplaas Cave, South Africa, provide increased resolution on late/terminal Pleistocene human behavioural variability. AZANIA. 2018;53(2):156–184. https://doi.org/10.1080/0067270X.2018.1436740

29. Clark AMB. The MSA/LSA transition in Southern Africa: New technological evidence from Rose Cottage Cave. S Afr Archaeol Bull. 1997;52:113–121. https://doi.org/10.2307/3889076

30. McCall GS, Thomas JT. Re-examining the South African Middle-to-Later Stone Age transition: Multivariate analysis of the Umhlatuzana and Rose Cottage Cave stone tool assemblages. AZANIA. 2009;44:311–330. https://doi.org/10.1080/00672700903337519

31. Wadley L. A typological study of the final Middle Stone Age stone tools from Sibudu Cave, KwaZulu-Natal. S Afr Archaeol Bull. 2005;60(182):51–63.

32. Kaplan J. The Umhlatuzana rock shelter sequence: 100 000 years of Stone Age history. South Afr Humanit. 1990;2:1–94.

33. Mohapi M. The Middle Stone Age point assemblage from Umhlatuzana rock shelter: A morphometric study. South Afr Humanit. 2013;25:25–51.

34. Sifogeorgaki I, Klinkenberg V, Esteban I, Murungi M, Carr AS, van den Brink VB. New excavations at Umhlatuzana Rockshelter, KwaZulu-Natal, South Africa: A stratigraphic and taphonomic evaluation. Afr Archaeol Rev. 2020;37:551–578. https://doi.org/10.1007/s10437-020-09410-w

35. Jacobs Z, Wintle AG, Duller GAT, Roberts RG, Wadley L. New ages for the post-Howiesons Poort, late and final Middle Stone Age at Sibudu, South Africa. J Archaeol Sci. 2008;35(7):1790–1807. https://doi.org/10.1016/j.jas.2007.11.028

36. Villa P, Delagnes A, Wadley L. A late Middle Stone Age artifact assemblage from Sibudu (KwaZulu-Natal): Comparisons with the European Middle Paleolithic. J Archaeol Sci. 2005;32(3):399–422. https://doi.org/10.1016/j.jas.2004.11.007